J Mater Sci (2009) 44:3235–3240
DOI 10.1007/s10853-009-3433-8

Structural and electronic properties of tellurite glasses

Simona Rada · Eugen Culea · Marius Rada · Petru Pascuta · Vistrian Maties

Received: 27 August 2008 / Accepted: 20 March 2009 / Published online: 10 April 2009

Abstract The structural properties of some tellurite glasses were investigated by FT-IR spectroscopy, density measurements, and quantum chemical calculations. Main results reveal that the ratio TeO_4/TeO_3 is found to decrease in the order $V_2O_5 > B_2O_3 > P_2O_5$. For borate–tellurate glasses, the Van Hove singularities corresponding to Te 5s orbital-derived states are cleft suggesting that there are strong tellurium–oxygen interactions. On the other hand, a strong effect of TeO_2 on the vitreous B_2O_3 network is also demonstrated by FT-IR spectrum. This effect yields the apparition of small peaks in the region ranges between 800 and 1600 cm^{-1} and probably the partial crystallization of the sample. Its spectral features are due to the B–O bond stretching of $[BO_4]$ and $[BO_3]$ structural units. The quantum chemical data obtained by us show that phosphate–tellurite and vanado–tellurate glasses can behave as semiconductors, whereas borate–tellurite glasses as insulators because the gap between the valence and conduction bands is >3 eV.

Introduction

Conventional oxides such as SiO_2, B_2O_3, and P_2O_5 can form glasses either alone or when mixed with considerable quantities of non-glass-forming oxides [1]. The physical characteristics of the phosphate glasses are different when compared to the silicates and the borates [2, 3]. Phosphate glasses have considerable potential for application in optical data transmission, solid-state batteries, and laser technologies, but their relatively poor chemical durability makes them generally unsuitable for practical applications [4].

Tellurite glasses [5, 6] are of technical interest because of their low melting points and absence of the hygroscopic properties which limit application of phosphate and borate glasses. Previous studies showed that vanadium tellurite glasses are semiconductors and that they switch when a high electrical field is applied [7, 8].

In this study, several physical properties of glasses were studied according to the formula $7TeO_2 \cdot 3M_2O_3$ and $7TeO_2 \cdot 3M'_2O_5$ (mol%), where M = B and M′ = P, V. The physical properties measured for this study include density and FT-IR spectroscopy. Special attention was paid to the relation between structure and electronic properties of the present glasses that exhibit a semiconductor behavior.

Experimental

The glasses were prepared from reagent grade TeO_2, H_3BO_3, P_2O_5, and V_2O_5. The mixture was melted in corundum crucibles in an electric furnace. The binary $7TeO_2 \cdot 3B_2O_3$ glassy was obtained when the crucible was transferred to a furnace for 60 min at 800 °C. For the preparation of the $7TeO_2 \cdot 3P_2O_5$ glassy was required temperature of 1100 °C and a time of 30 min. Sample with $7TeO_2 \cdot 3V_2O_5$ composition was prepared in a furnace at 850 °C for 10 min.

The samples were analyzed by means of X-ray diffraction (XRD) using a XRD-6000 Shimadzu Diffractometer,

S. Rada (✉) · E. Culea · P. Pascuta
Department of Physics, Technical University of Cluj-Napoca, 400641 Cluj-Napoca, Romania
e-mail: Simona.Rada@phys.utcluj.ro; radasimona@yahoo.com

M. Rada · V. Maties
Department of Mechatronic, Technical University of Cluj-Napoca, 400641 Cluj-Napoca, Romania

with a monochromator of graphite for Cu-Kα radiation ($\lambda = 1.54$ Å) at room temperature.

The FT-IR absorption spectra of the studied glasses were measured for each glass sample over the range of 400 to 1600 cm^{-1} wavenumber. A JASCO FTIR 6200 spectrometer was used in conjunction with the potassium bromide, disk technique. Samples of glass weighing 0.002 g were mixed and ground with 0.300 g KBr. After which the mixture was pressed at 10 tons for 3 min under vacuum, to yield transparent disks suitable for mounting in the spectrometer. The precision of the absorption band maxima is ± 2 cm^{-1}.

The density of a glass for each composition was evaluated by the Archimedes method using water as an immersion liquid.

The starting structures have been built using the graphical interface of Spartan'04 software [9] and preoptimized by molecular mechanics. Optimizations were continued at density functional theory (DFT) level. The DFT computations were performed with B3PW91/CEP-4G/ECP method using Gaussian'98 package of programs [10].

It should be noticed that only the broken bonds at the model boundary were terminated by hydrogen atoms. The positions of boundary atoms were frozen during a calculation and the coordinates of internal atoms were optimized, to model the active fragment flexibility and its incorporation into the bulk.

Frequency analysis followed all optimizations in order to establish the nature of the stationary points found, so that all the structures reported in this study are genuine minima on the potential energy surface at this level of theory, without any imaginary frequencies.

After inferring the equilibrium configuration of the studied glasses models, we calculated the densities of states (DOS) by the extended Hückel tight-binding method using the BICON-CEDIT package [11].

Results and discussion

FT-IR spectroscopy

The XRD patterns obtained did not reveal any crystalline phase in the samples (Fig. 1).

The experimental IR spectra of $7TeO_2 \cdot 3M_2O_3$ and $7TeO_2 \cdot 3M'_2O_5$, where M = B and M′ = P, V glass system were presented in Fig. 2. Because the majority of the bands are very broad and asymmetric, presenting also some shoulders, a deconvolution of the experimental spectra was necessary.

This deconvolution allowed us a better identification of all bands that appear in the FT-IR spectra to realize their

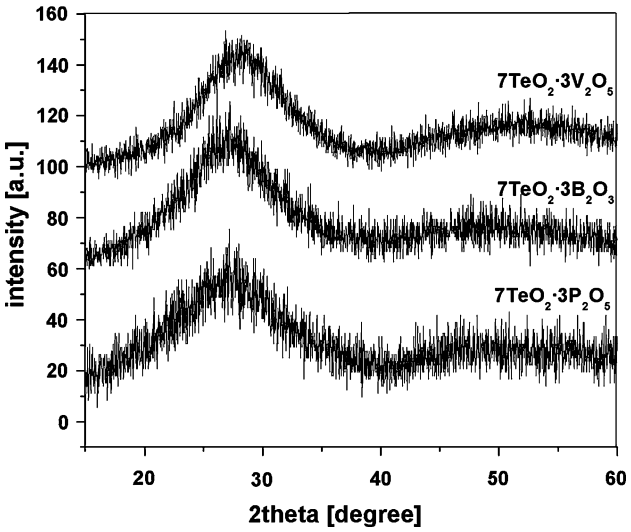

Fig. 1 XRD pattern for studied glasses

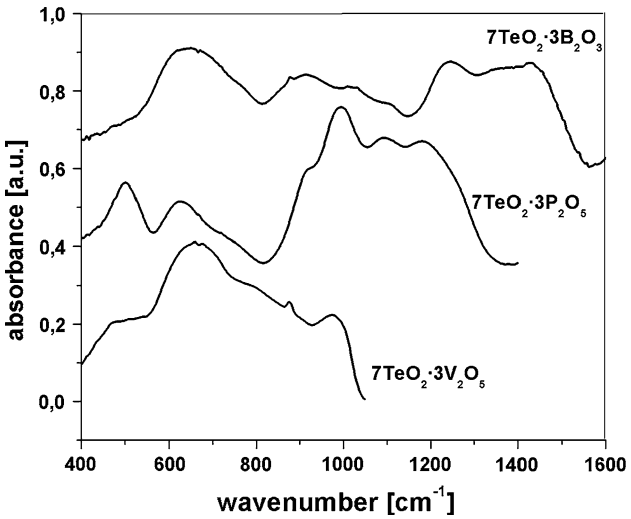

Fig. 2 FT-IR spectra of the studied glasses

assignment. The proportion of the particular structures corresponding to different vibration modes was calculated from the areas of fitter Gaussian bands divided to the total areas of these bands. Each component band is related to some types of vibration in specific structural groups. The concentration of the structural group was considered to be proportional to the relative area of its component band [12]. The deconvolution parameters, the band centers, *C*, and the relative area, *A*, as well as the bands assignment for the studied glass are given in Table 1.

The observed FT-IR bands for the presently investigated binary tellurite–vanadate glasses are assigned to the Te–O linkage vibration in $[TeO_4]$, $[TeO_3]$ units, and the V–O linkage vibration in $[VO_4]$, $[VO_5]$ units (Fig. 3a).

The bands appear around 495 cm^{-1}, in the 610–680 and 720–780 cm^{-1} range are assigned the bending mode of

Table 1 Deconvolution parameters (the band centers, *C*, and the relative area, *A*,) and the bands assignments for the studied glasses

$7TeO_2 \cdot 3V_2O_5$		$7TeO_2 \cdot 3B_2O_3$		$7TeO_2 \cdot 3P_2O_5$		Assignments
C	*A*	*C*	*A*	*C*	*A*	
495	26.5	474	25.7	495	43.4	Bending vibrations of Te–O–Te or O–Te–O linkages
620	17.7	621	33.5	625	18.5	Stretching vibrations [TeO_4]
680	15.2					Stretching vibrations [TeO_4]
780	29.8	726	31.8	720	18.8	Stretching vibrations [TeO_3]
907	15.1					Stretching vibrations [VO_5]
988	8.0					Stretching vibrations [VO_4]
		904	45.0			B–O stretching vibrations in BO_4 units
		1058	27.11			B–O stretching vibrations in BO_4 units
		1251	47.8			B–O stretching vibrations in BO_3 units from boroxol rings
		1423	46.1			$B–O^-$ stretching vibrations in BO_3 units from varied types of borate groups
				987	113.1	[PO_4] of orthophosphate
				1122	41.8	PO_2 of metaphosphate groups
				1222	64	P=O stretchings of PO_2 groups

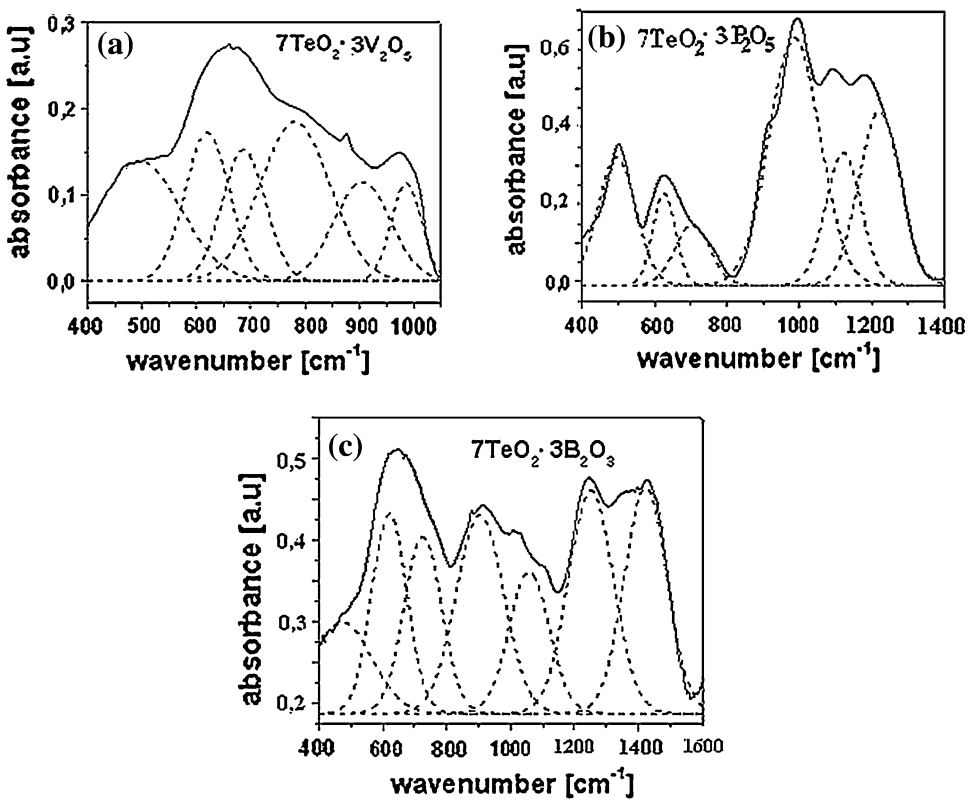

Fig. 3 The experimental and deconvolution FT-IR spectra for the **a** $7TeO_2 \cdot 3V_2O_5$, **b** $7TeO_2 \cdot 3P_2O_5$, and **c** $7TeO_2 \cdot 3B_2O_3$ system

Te–O–Te or O–Te–O linkages, the stretching mode [TeO_4] trigonal pyramidal with bridging oxygen and the stretching mode of [TeO_3] trigonal pyramidal with non-bridging oxygen, respectively [6, 8, 13].

In the case of pure V_2O_5 glass, it has been reported [14] that V^{+5} ions exhibit both four and five-fold coordination states, depending on the sample preparation conditions. The IR spectrum of pure crystalline and amorphous V_2O_5 is characterized by the intense band in the range 1000–1020 cm^{-1}, related to the vibration of isolated V=O vanadyl groups in [VO_5] trigonal bipyramids [15–17]; the band located in the range 850–910 cm^{-1} corresponding to the

vibrations of [VO_5] units, whereas the band located in the range 950–988 cm^{-1} was attributed to [VO_4] units [18–20].

The IR spectra and their deconvolution of the $7TeO_2 \cdot 3P_2O_5$ glass sample are shown in Fig. 3b. The main features of IR spectra are six bands at ~495, 625, 720, 987, 1122, and 1222 cm^{-1}, respectively, due to different structural units.

The bands located at about 625 and 720 cm^{-1} are identified to be due to the vibrations of [TeO_4] and [TeO_3] units, respectively. In the FT-IR spectra, a prominent band at 987 cm^{-1} is attributed to the symmetric stretching vibration of [PO_4] of orthophosphate groups [21, 22]. The shoulder near ~900 cm^{-1} is assigned to the asymmetric stretching mode [23]. The position of band from ~1100 cm^{-1} corresponds to the vibrations of PO_2 of metaphosphate groups. The band centered at ~1175 cm^{-1} is assigned to the PO_2 symmetric stretching mode and P–O–P of [PO_4] tetrahedral sharing corners. The band at 1122 cm^{-1} is identified due to the vibrations of PO_2 of metaphosphate groups and a band centered in the region 1222 cm^{-1} is due to P=O stretchings [24]. The low-frequency absorption band at 540 cm^{-1} is assigned to harmonics of bending vibration O=P–O linkages [25]. This band appears in most binary and ternary phosphate glasses [26].

The intensity of the band at 987 cm^{-1} related to the [PO_4] groups in orthophosphate structure indicating an increase in the number of non-bridging oxygen due to depolymerization of the glass network [27].

The spectrum of $7TeO_2 \cdot 3B_2O_3$ glass is presented in Fig. 3c. The broadband at 650 cm^{-1} is the envelope of the two characteristic bands (621 and 726 cm^{-1}) and they are attributed to the stretching vibration between tellurium and non-bridging oxygen atoms like in trigonal bipyramid [TeO_3] or polyhedra [TeO_{3+1}] groups [28]. Some authors consider that the shoulder at 780 cm^{-1} can be due to a more distorted [TeO_4] groups than in TeO_2 reference crystals [26] or the benefit of the one of [TeO_3] entities [29].

The region ranges between 800 and 1200 cm^{-1} and its spectral features are due to the B–O bond stretching of tetrahedral BO_4 units [30, 31]. The large absorption band in the 820–1150 cm^{-1} spectral region is splitting into two components at 940 and 1058 cm^{-1}. All these bands are attributed to the stretching vibration in [BO_4] units [30]. The band centered at ~1251 cm^{-1} is attributed to B–O stretching vibrations in [BO_3] units from boroxol rings [31]. The band at 1423 cm^{-1} is assigned to the $B–O^-$ stretching vibrations in [BO_3] units from varied types of borate groups [32].

The peak assignments of the deconvolution IR spectra for studied glasses are given in Table 1. The relative area ratio of [TeO_4] and [TeO_3] units hereafter referred as TeO_4/TeO_3 represents ratio of [TeO_4] and [TeO_3] structural units [33]. The variation of relative area ratio with M_2O_3 or M_2O_5 content is illustrated in Table 2. In general, the ratio TeO_4/TeO_3 is found to decrease in the order $V_2O_5 > B_2O_3 > P_2O_5$ and indicating the transformation of [TeO_4] in [TeO_3] units.

Density and molar volume data

The density of glasses is of special importance in the context of the study of their structure. Thus, such importance arises when the density of a glass shows a non-linear compositional dependence because this behavior suggests structural changes produced by compositional modifications.

Table 2 shows the variation of density as function of the metal oxide content of the studied glasses. The estimated error for the determined density values was <0.2 g cm^{-3}.

For $7TeO_2 \cdot 3V_2O_5$ and $7TeO_2 \cdot 3B_2O_3$ glasses, the density decreases with the increase molecular weight of the glass which could be explained by considering some conversion of [TeO_3] into [TeO_4] units, which will lead to the open structure of the glasses. The density increases abruptly when phosphorus oxide was added in the tellurite glass network. This could be explained by considering that the molecular weight of the phosphate–tellurite glasses was increased due to their hydroscopic properties.

The molar volume is of high interest, because it is directly related to the spatial distribution of the oxygen in the glass network. The substitution of B_2O_3 by V_2O_5 or P_2O_5 in the glass matrix may lead to the increase in the molar volume because the molecular volume of V_2O_5 and P_2O_5 are larger than that of the B_2O_3. The observed decrease in the molar volume may be attributed to a decrease in bonds' length or/and inter-atomic spacing between atoms, too. This important result is in agreement with the decrease in the ratio [TeO_4]/[TeO_3] evidenced by the IR data.

Density of states

The resulted IR data were used in this research in order to compute the possible structural models of the studied

Table 2 The relative area ratio of TeO_4/TO_3, the density, and molar volume of the studied glasses

Glass	$7TeO_2 \cdot 3V_2O_5$	$7TeO_2 \cdot 3B_2O_3$	$7TeO_2 \cdot 3P_2O_5$
Density (g cm^{-3})	4.22	4.96	5.64
Molar volume (cm^3 mol^{-3})	393.7	267.3	273.5
TeO_4/TeO_3	1.1	1.05	0.98

glasses. The fully optimized models obtained by performing DFT calculations were used to compute the DOS. Similar methodology has previously been reported to study other glasses [34–37].

If one define DOS(E)dE as the number of one-electron levels in the infinitesimal interval dE, then the total density of state is DOS(E) = $\sum_i \delta(E - e_i)$ (where δ is the Dirac function and e_i stands for the one electron energies). Partial DOS reveals the specific contribution of an atomic orbital χ_μ to one-electron levels at certain energies. The energy difference between the bottom of the conduction band and the top of the valence band in a semiconductor or in an insulator is called the band gap energy, E_g.

The data obtained by us show that phosphate–tellurite and vanadate–tellurite glasses can behave as semiconductors and borate–tellurite glasses as insulators. From the partial DOS(E) plot for borate–tellurite glasses shown in Fig. 4a, we can specify that the lowest band (valence band) is composed of O(2s)-derived states, while the conduction bands are composed of ns orbitals of tellurium, boron, and oxygen mixed with the np orbitals of tellurium and boron, respectively. The bandwidth of the band gap provides a distinction between a semiconductor and an insulator. Since the gap between the valence and conduction bands is >3 eV, it indicates that this glass has insulator behavior [23, 33, 34]. The Van Hove singularities corresponding to tellurium orbital-derived states are cleft, which to show that there are strong tellurium–oxygen interactions.

The results obtained for phosphate–tellurite glasses are revealed in Fig. 4b. The dashed horizontal line represents the Fermi level. Three main regions can be observed in the total DOS: the lowest region below −26 eV mainly corresponds to the occupied O 2s states, which are well separated by 2 eV from occupied Te 5p states. The next region under Fermi level has contributions also from O (2p)-derived states and admixture of Te (5s, 5p), O(2p), and P (3s, 3p) orbitals. The conduction bands consist the mixture of P(3p), Te(5 s, 5p), and O(2p)-derived states.

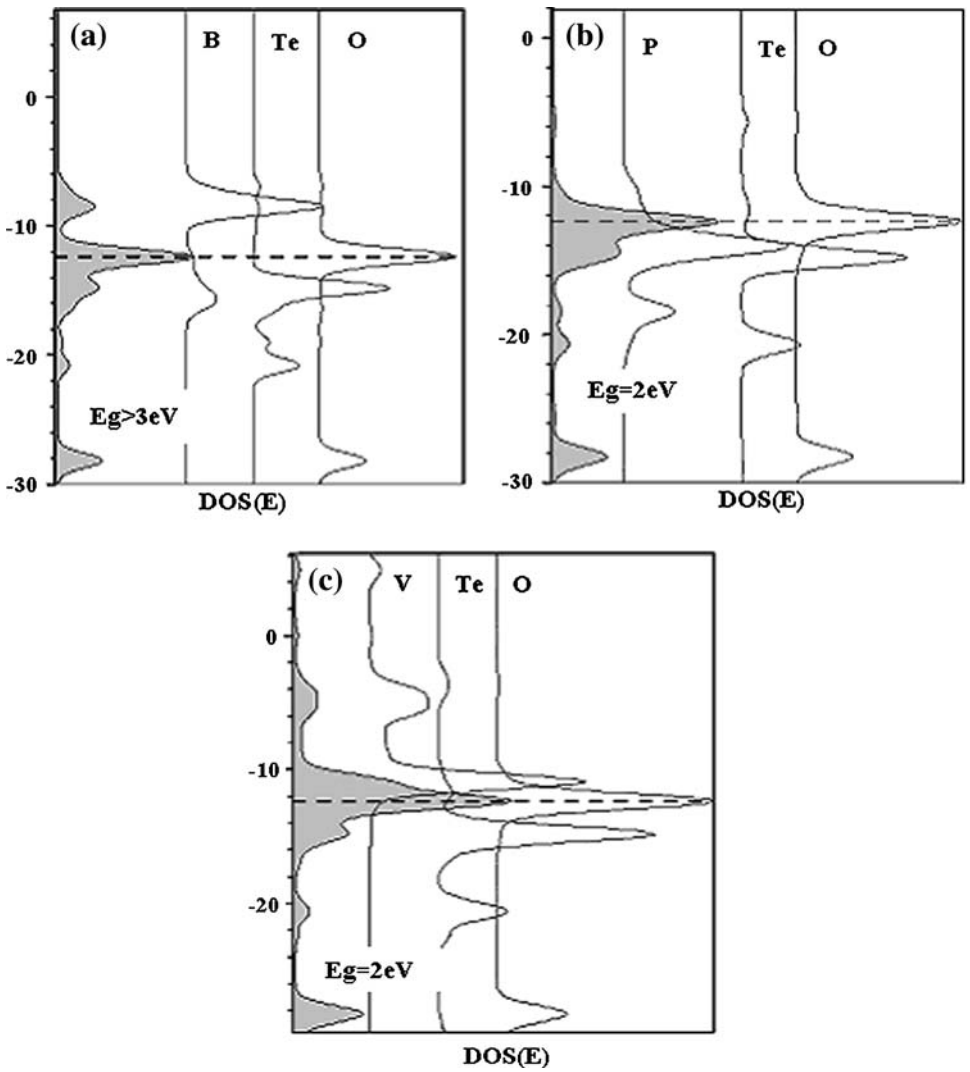

Fig. 4 The total and partial DOS diagrams of the:
a $7TeO_2 \cdot 3B_2O_3$;
b $7TeO_2 \cdot 3P_2O_5$;
c $7TeO_2 \cdot 3V_2O_5$ glass

For vanadate–tellurite glasses, the partial DOS(E) plot shows that the conduction band regions under Fermi level correspond to the O 2p states mixed with 5s, 5p orbitals of the Te, 4s V states and that above Fermi level is composed of V(4s, 4p, 3d), Te(5s, 5p), and O(2p)-derived states (Fig. 4c).

The Fermi level is located in the middle of Van Hove singularities corresponding to O p-orbital-derived states. This is considered as an indication that there is overlap with oxygen orbitals [38]. For borate–tellurate glasses, the Van Hove singularities corresponding to Te 5s orbital-derived states are cleft, suggesting that there are strong tellurium–oxygen interactions. On the other hand, a strong effect of TeO_2 on the vitreous B_2O_3 network is also demonstrated of FT-IR spectrum. This effect yields the apparition of small peaks in the region ranges between 800 and 1600 cm^{-1} and probably the partial crystallization of the sample. Its spectral features are due to the B–O bond stretching of [BO_4] and [BO_3] structural units.

Conclusions

The XRD and FT-IR spectra for glass containing $7TeO_2 \cdot 3M_2O_5$ (M = P, V) and $7TeO_2 \cdot 3B_2O_3$ compositions have been investigated in order to understand their structural properties. The addition of B_2O_3 content in the composition of tellurite glass leads to an increase in [TeO_4] and to the open structure of the glasses.

Calculations on their basic electronic properties show that the borate–tellurite glasses are insulators, whereas the phosphate–tellurite and vanadate–tellurite glasses have semiconductor properties.

For borate–tellurate glasses, the Van Hove singularities corresponding to tellurium orbital-derived states are cleft, suggesting that there are strong tellurium–oxygen interactions. This agrees the results of the FT-IR spectra that show the presence of small peaks in the spectral features of the B–O bond vibration of [BO_4] and [BO_3] structural units.

References

1. West AR (1984) Solid state chemistry and its applications. Wiley, New York, p 592
2. He Y, Day DE (1992) Glass Technol 33:214
3. Sidek HAA, Collier IT, Hampton RN, Saunders GA, Bridge B (1989) Philos Mag 59B:221
4. Yung H, Shih PY, Liu HS (1997) J Am Ceram Soc 80:2213
5. Rada S, Culea E, Culea M (2008) J Mater Sci 43(19):6480. doi: 10.1007/s10853-008-2980-8
6. Rada S, Culea E, Rus V, Pica M, Culea M (2008) J Mater Sci 43(10):3713. doi:10.1007/s10853-008-2601-6
7. Gaman VI, Peznikov VA, Fedyainova NI, Vyssh UZV (1972) Zaved Fiz 2:57
8. Sidkey MA, El Mallawany R, Nakhla RI, Abd El-Moneim A (1997) J Non-Cryst Solids 215:75
9. Spartan'04 Software, Wavefunction Inc., Irvine, CA
10. Frisch MJ, Trucks GW, Schlegel HB, Scuseria GE, Robb MA, Cheeseman JR, Zakrzewski VG, Montgomery JA, Stratmann RE, Burant JC, Dapprich S, Millam JM, Daniels AD, Kudin KN, Strain MC, Farkas O, Tomasi J, Barone V, Cossi M, Cammi R, Mennucci B, Pomelli C, Adamo C, Clifford S, Ochterski J, Petersson GA, Ayala PY, Cui Q, Morokuma K, Rega N, Salvador P, Dannenberg JJ, Malick DK, Rabuck AD, Raghavachari K, Foresman JB, Cioslowski J, Ortiz JV, Baboul AG, Stefanov BB, Liu G, Liashenko A, Piskorz P, Komaromi I, Gomperts R, Martin RL, Fox DJ, Keith T, Al-Laham MA, Peng CY, Nanayakkara A, Challocombe M, Gill PMW, Johnson B, Chen W, Wong MW, Andres JL, Gonzales C, Head-Gordon M, Replogle ES, Pople JA (1998) Gaussian 98 Rev A.5 Programme. Gaussian Inc., Pittsburgh, PA
11. Brandle M, Rytz R, Calzaferri G (1997) BICON-CEDIT Software. University of Bern, Switzerland
12. Ganguli M, Rao KJ (1999) J Solid State Chem 145:65
13. Shaltout I, Tang Y, Braunstein R, Abu-Elazm AM (1995) J Phys Chem Solids 56:141
14. Mendialdua J, Casanova R, Barbaux Y (1995) J Electron Spectrosc Relat Phenom 71:249
15. Miyata H, Fujii K, Ono T, Kubokawa Y, Ohno T, Hatayama F (1987) J Chem Soc Faraday Trans 83:675
16. Dimitrov V (1987) J Solid State Chem 66:256
17. Khattak GD, Tabet N, Wenger LE (2005) Phys Rev 72B:104203
18. de Waal D, Hutter C (1994) Mater Res Bull 29:843
19. Manara D, Grandjean A, Pinet O, Dussossoy JL, Neuville DR (2007) J Non-Cryst Solids 353:12
20. Anderson GW, Compton WD (1970) J Chem Phys 52:6166
21. Janakirama Rao BHV (1965) J Am Ceram Soc 48:311
22. Efimov AM (1997) J Non-Cryst Solids 209:209
23. Rada S, Culea M, Culea E (2008) J Phys Chem A 112(44):11251
24. Doweidar H, Mostafa YM, El-Egili K, Abbass I (2005) Vib Spectrosc 37:91
25. Shin PY, Yung SW, Chin JS (1999) J Non-Cryst Solids 249:1
26. Abid M, Et-labirou M, Taibi M (2003) Mater Sci Eng 97B:20
27. Sabadel JC, Armand P, Cachau-Herreillat D, Baldeck P, Doclot O, Ibanez A, Philippot E (1997) J Solid State Chem 132:411
28. Fargin E, Berthereau A, Cardinal T, Le Flem G, Ducase L, Canioni L, Segonds P, Sarger L, Ducasse A (1996) J Non-Cryst Solids 203:96
29. Dwivedi BP, Rahman MH, Kumar Y, Khanna BN (1993) J Phys Chem Solids 54:621
30. Pascuta P, Pop L, Rada S, Bosca M, Culea E (2008) J Mater Sci Mater Electron 19(5):424
31. Rada S, Culea M, Neumann M, Culea E (2008) Chem Phys Lett 460(1–3):196
32. Himei Y, Osaka A, Nanba T, Miura Y (1994) J Non-Cryst Solids 177:164
33. Rada S, Pascuta P, Bosca M, Culea M, Pop L, Culea E (2008) Vib Spectrosc 48(2):255
34. Rada S, Culea E, Rus V (2008) J Mater Sci 43(18):6094. doi: 10.1007/s10853-008-2949-7
35. Greenham NC, Friend RH (1995) In: Ehrenreich H, Spaepen F (eds) Advances in research and application, vol 49. Academic Press, New York, p 1
36. Rada S, Culea E, Bosca M, Culea M, Muntean R, Pascuta P (2008) Vib Spectrosc 48(2):285
37. Rada S, Culea M, Culea E (2008) J Non-Cryst Solids 354(52–54): 5491
38. Cappelutti E, Pietronero L (1996) Europhys Chem 36:619